

## Presenting an experimental creep model for rock salt

M.B. Eslami Andargoli<sup>1</sup>, K. Shahriar<sup>2\*</sup>, A. Ramezanzadeh<sup>3</sup> and K. Goshtasbi<sup>4</sup>

1. Department of Mining Engineering, Science and Research Branch, Islamic Azad University, Tehran, Iran
2. Department of Mining and Metallurgy Engineering, Amir Kabir University of Technology, Tehran, Iran
3. Faculty of Mining, Petroleum & Geophysics Engineering, Shahrood University of Technology, Shahrood, Iran
4. Department of Mining Engineering, Tarbiat Modares University, Tehran, Iran

Received 20 December 2017; received in revised form 25 March 2018; accepted 5 May 2018

\*Corresponding author: k.shahriar@aut.ac.ir (K. Shahriar).

### Abstract

During the recent decades, the design and construction of underground spaces into rock salt have been particularly regarded for storing petroleum fluids, natural gas, and compressed air energy, and also for disposing nuclear and chemical wastes. The rock salt hosting such spaces will be subjected to various types of monotonic/cyclic, short-term/long-term stresses during the construction and/or operation phases. On this basis, it is necessary to investigate the mechanical behavior of the rock salt under the effects of various monotonic short-term/long-term stresses. Out of the most important factors affecting the creep behavior of rock salt are the composition of minerals and size of the crystals comprising the rock salt, humidity, temperature, time, loading scheme, loading rate, strain rate, and loading period. In the present research work, a loading scheme and a loading period were considered. On this basis, in order to achieve a true understanding of the creep behavior of rock salt, it is necessary to determine the creeping coefficients via laboratory tests. Thus, twenty cylindrical (length to diameter ratio  $> 2$ ) specimens of rock salt were prepared for conducting the creep tests. Two stepwise short-term creep tests (each at three stress levels, namely 4.4, 10.1, and 11.9 MPa, and 7.5, 12, and 17 MPa, respectively) and eighteen long-term creep tests (at six stress levels, namely 5.5, 7.5, 10, 12, 14, and 18 MPa) were conducted. Then, first, the creep coefficients were determined according to the Lubby 2 constitutive model. These coefficients were adjusted using the results of the creep tests. Afterwards, a creep experimental model was presented using linear and nonlinear regression of the creep test data. For validation of the results obtained, both the adjusted Lubby 2 constitutive model and the proposed experimental model were compared with the results obtained for the creep tests. Both models had fairly good agreements with the data for the creep tests at a determination factor of about 93%.

**Keywords:** *Rock Salt, Creep Test, Experimental Model, Lubby 2 Model, Creep Coefficients.*

### 1. Introduction

Rock salt exhibits complex mechanical behaviors in different conditions. Given the extensive application of rock salt in the construction and development of large-scale underground caverns storing strategic fluids, buried nuclear waste, stope pillars, and mining tunnels, many studies have been performed on the properties and behavior of this rock material. Previous investigations show that such parameters as the stress level, loading or unloading rate, temperature, humidity, and grain size affect the

rock salt behavior significantly. Studies on rock salt deformation show that the rock exhibits different behaviors in different stress fields [1, 2]. Material scientists believe that the rock salt behavior is similar to those of metals and ceramics but with significant differences. Deformations of rock salt can be studied from two aspects. On one hand, similar to many other natural materials such as rocks, salt crystals may exhibit a brittle behavior in specific conditions. On the other hand, resembling metals, ceramics, and minerals, salt

rock exhibits a ductile behavior (elastic deformations with minimum or no fracture development) in low strains and under medium-to-high stresses. A major property of a ductile material (e.g. salt) is that it shows a strain-hardening behavior under deviatoric stress fields at temperatures below 50% of its melting point [3-5].

In general, a time-dependent deformation or creep is a process where rock deformation continues with no change in stress. The creep behavior of rock salt can be classified into three stages, namely transient, steady-state, and accelerating creep behaviors (Figure 1). The time duration of the transient stage is very short, and it is solely considered in research work studies. The other two stages and their effective factors are, however, important in the design and stability of underground spaces [6].

Figure 1 shows a typical creep curve in strain-time, which consists of four parts. The first

part relates to an elastic or instantaneous strain that results from immediate load or stress (vertical yellow line). The second part is related to the primary or transient creep. In this section, by removing the load or stress, first the elastic strain is immediately restored, the restoration process continues, and the strain remains with zero over time (blue curve). In this section, the strain rate decreases exponentially. The third part is the secondary or steady-state creep, where a permanent deformation occurs. The strain rate in this section is constant, and the strain or deformation is asymptotically reached to a certain value (red line). The fourth part relates to the tertiary or accelerated creep, which increases to a failure point at an incremental rate, and the specimen develops a sudden failure (green line). Therefore, the total strain at the instant of failure is equal to the sum of the elastic strain ( $\epsilon_e$ ), the primary creep ( $\epsilon_{Pr}$ ), the secondary creep ( $\epsilon_{Se}$ ) and the third stage creep ( $\epsilon_{Te}$ ) [4-6].

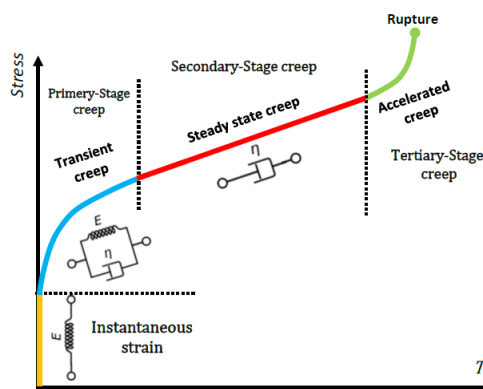


Figure 1. A typical creep deformation under constant stress [5].

The constitutive models presented for description of the creep behavior of rock salt indicate that the ductile behavior is dependent on factors such as the loading type [7, 8], loading rate [9], crystal size and contact between crystals [4, 10], time [11, 12], temperature [13, 14], humidity [15, 16], inclusions [17], and stress history [18-20]. Each one of these factors affects the time-dependent behavior of rock salt. In this research work, among the mentioned factors, the effect of the history of stress on the creep coefficients was investigated.

The constitutive laws of creep behavior of rock salt are based upon the results obtained from experiments, and serve essentially as a method for fitting some mathematical functions to the experimental data. However, not all of these models are based on a specific theory. In general, the 1D constitutive laws can be divided into two groups: intuitive models and rheological ones. In

cases where rock behavior results in an irreversible or permanent strain, the non-linear rheological models are often the models of choice [6, 27]. Therefore, in all the constitutive creep models for rock salt, it is necessary to determine the most important time-dependent parameters including the viscoelastic and viscoplastic coefficients.

Many models are presented to simulate the behavior of rock salt in each one of the creep stages referred to in Figure 1. Since it seeks to ensure a proper safety in the operating conditions of oil and gas liquid storage caverns as well as rock salt mines, most of the models presented in the range of primary and secondary creep have been concentrated [21- 23]. However, there are few models that simulate the third stage of creep [24-27]. Some of these models are empirically based upon laboratory tests and the others are rheologically based upon mechanical elements.

Each one of these models will be explained in more detail.

### 1.1. Experimental models

In this category of methods, experimental tests are performed to measure sample deformation followed by vertical and lateral strains within specific time intervals under the test conditions. Subsequently, the results obtained are used to plot strain vs. time curves. These curves are modeled using nonlinear mathematical functions and will be capable of modeling both the transient and the stable creeps. In the empirical methods, the general equation used for strain rate has the form of Eq. (1):

$$\dot{\varepsilon} = F(t) \cdot \sigma^n \cdot T \quad (1)$$

In this equation, strain rate  $\dot{\varepsilon}$  is defined on the basis of a decreasing function  $F(t)$ , temperature  $T$ , stress  $\sigma$  and  $n^{\text{th}}$  power of the applied stress. The exponent  $n$  depends on the tested rock type. The design and execution of experimental tests in empirical methods is a very costly and time-consuming task. Therefore, using other methods alongside the empirical ones will help generalize the results of experimental tests to long-term intervals. As of now, numerous empirical models have been presented, most of which have presented almost similar definitions for the creep behavior of material [2, 6, 15, 22, 23].

### 1.2. Rheological models

In these methods, the creep behavior of rock is described using the mechanical models resembling the behavior of the considered rock. These models are composed of springs, dampers, and sliders, the combination of which can justify the elastic, viscoelastic, and viscoplastic deformations of the rock. Each one of the rheological methods has been developed under a specific set of conditions in terms of temperature, confining pressure, and deviatoric stress fields. As such, it is extremely difficult to achieve an accurate solution using such models in complicated cases. In such cases, numerical methods will be helpful. The models developed using this method are called constitutive laws. As of current, numerous constitutive laws have been derived from the original models, as detailed in various references [4, 5].

Many of these models are related to metals, but are also used for crystalline material. These relationships have been defined by assuming an

isotropic structure for the material and constrained deformations. The general framework of these models is presented as Eq. (2):

$$\dot{\varepsilon} = F_{(A, \sigma, T, \varepsilon, Z_i)} \exp\left(\frac{-Q}{RT}\right) \quad (2)$$

where  $\dot{\varepsilon}$  is the strain rate,  $F$  is a function,  $A$  is the material constant,  $\sigma$  is the stress field,  $T$  is the absolute temperature,  $\varepsilon$  is the strain,  $Z_i$  takes into account other factors such as humidity and impurities,  $Q$  is the activation energy, and  $R$  is the universal gas constant [1, 15, 23, 27].

In this research work, first, the creep coefficients are determined based on the Lubby 2 constitutive model and the Burger's rheological model. Then these coefficients are adjusted based on the creep tests. An experimental creep model is also proposed based on the creep test data. The proposed experimental creep model was created by trial and error to best match the experimental test data. The experimental creep model is compared with the modified Lubby 2 model in order to obtain an accurate understanding of the creeping behavior of the studied rock salt. The studied rock salt is from Khoshkalat mine located in Garmsar County, Semnan province, Iran.

## 2. Experimental tests

### 2.1. Preparing specimens

The rock salt samples used in the present research work were from Khoshkalat Salt Mine in Garmsar town in the Semnan Province, Iran. The mine is located 28 Km to the west of the Garmsar town and is mined via the room and pillar method. Obtaining cylindrical specimens of rock salt via the conventional sampling methods is associated with particular problems, as compared to other hard rocks. The required specimens were taken using the dry method by injecting compressed air instead of saturated brine.

In air-assisted coring, air was pumped by a CB 100 compressor operating at 100 lit/min and 10 bar. Undertaking a series of experiments, the optimal core barrel rpm and the rate of penetration (ROP) were obtained as 3000 rpm and 0.55 cm/min, respectively. All of the cores were prepared under ambient conditions (a temperature of 20 °C and a relative humidity of 27%). The obtained cores were cut and flattened before being wrapped in humidity-insulated aluminum sheets to keep them as undisturbed as possible against changes due to humidity and other environmental factors. Figure 2 shows the core machine and a number of the prepared cores from rock salt. The prepared rock salt specimens were composed of

halite (97%) and minor impurities (less than 3%) including anhydrate and clay minerals. All specimens were prepared at length-to-diameter ratios in the range of 2.3-2.5.

The point to note is that in case the deformations are small or say strain is  $\varepsilon \leq 2\%$ , the strains can be calculated using the technical strain equation (Eq. (3)):

$$\varepsilon_t = \frac{\Delta l}{l_0} \times 100\% \quad (3)$$

where  $\varepsilon_t$  is the technical strain (in percentage),  $\Delta l$  is the measured axial deformation of the specimen (in mm), and  $l_0$  is the length of the unstressed specimen (in mm).

The other point to note is that in case the deformations are large, or say strain is  $\varepsilon \geq 2\%$ , the strains can be calculated using the true (logarithmic) strain equation (Eq. (4)) rather than the technical strain equation (Eq. (3)):

$$\varepsilon_{\ln} = \left| \int_{l_0}^l \frac{dl}{l} \right| 100\% = \left| \ln \frac{l}{l_0} \right| \times 100\% = |\ln(1 - \varepsilon_t)| \times 100\% \quad (4)$$

where  $\varepsilon_{\ln}$  is the true (logarithmic) strain (in percentage) and  $l$  is instantaneous length of the stressed specimen that is equal to  $l_0 - \Delta l$ . In the present research work, the technical strain relationship was used to calculate strain in short-term tests.

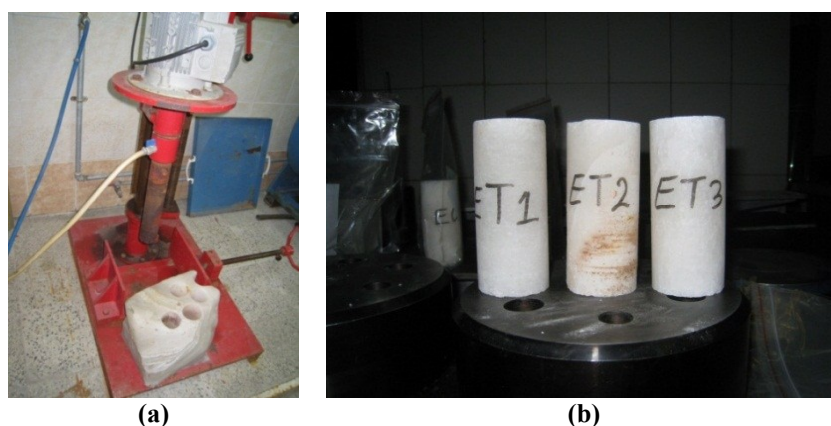


Figure 2. a) Coring machine connected to the compressor b) a number of prepared samples.

## 2.2. Uniaxial compressive strength test

In order to determine the basic mechanical characteristics of the rock salt, the uniaxial compressive strength (UCS) tests were performed on five core specimens. Table 1 presents the specifications of the tested cores. The tests were performed under the same set of laboratory environment conditions in terms of mean temperature (20 °C) and relative humidity (23%). The specimens were loaded using a MTS servo-control device.

In the UCS tests, given that the salt experiences not only elastic deformations, but also large inelastic strains, its static modulus of elasticity reduces significantly to as low as about 1.5 GPa. As such, this modulus is calculated using the cyclic loading tests where multiple cycles of loading are applied to the specimen. In the cyclic loading test, putting aside the initial and final cycles where the specimen undergoes large deformations, the cyclic loading imposes no influence on the elastic modulus of salt, so that the value of this modulus remains practically constant (10 GPa) throughout the test.

In order to determine the Poisson's ratio of the rock salt specimens, chain LVDT strain gauge was used to measure lateral strains in the UCS tests. Vertical displacements were measured and recorded using an electronic displacement sensor mounted on the loading jaw of the testing machine. Figure 3 demonstrates the configuration of lateral displacement sensors on the testing machine. Table 2 shows the results of the UCS test on the specimens.

## 2.3. Creep tests

Given that various underground spaces in salt domes and formations may be subjected to long-term uniform and cyclic loads depending on their application in the course of construction and operation phases, it seems necessary to study the rock salt properties under real conditions.

In the present research work, in order to determine the creep parameters, two methods were designed for conducting the creep test. The Long-Term Creep (LTC) tests were performed to determine the Maxwell's coefficient of viscosity, while the stepwise Short-Term Creep (STC) tests were

conducted to determine the Kelvin’s coefficients in a better and more accurate manner. Firstly, the LTC tests were performed under separate and different axial stresses, namely 5.5, 7.5, 10, 12, 14, and 18 MPa. For each one of the stress levels, at least three tests were carried out. According to the technical limitations and the test unit mechanism, the tests were performed within different time intervals. Considering the limitations in time and performance of the hydroelectric pump used in the creep test machine, the LTC tests were performed at different days. The properties of the rock salt samples used in LTC are brought in Table 3. For example, Figure 4 shows the results of some LTC tests in terms of the strain-time curves. However, in the LTC test under 10 MPa stresses, the results obtained exhibit some non-reasonable scattering, which is due to structural defects in the rock salt specimens and the operation mechanism of the creep test machine that tends to produce scattering in this test data. As it can be seen in Figure 4, instantaneous strain depends on the applied stress. Accordingly, the higher the level of the applied stress, the larger would be the instantaneous strain. Also the long-term creep tests under 14 and 18 MPa are fractured at the end of test.

Moreover, in order to obtain the viscoelastic coefficient, the stepwise STC tests were conducted on two cylindrical samples of the rock salt with the properties indicated in Table 4. Each one of these two tests was executed on the specimens at three stresses in the order of increasing, namely 4.4 MPa, 10.1 MPa, and 11.9 MPa, and also 7.5 MPa, 12 MPa, and 17 MPa. Each test was set to last for 6 hours. The considered stress in each test was applied to the specimen instantaneously and kept unchanged for two hours. In both tests, the stress level was increased when the specimen did not experience stable a creep for more than 1.5 hours. Figure 5 shows the results of stepwise STC in the form of strain-time diagrams. The results obtained from the experiments indicate that with increase in the level of stress, the amount of transient creep in the rock increased so that the stable creep phase entered at a steeper (or almost the same) slope. In other words, with increasing the level of stress, the creeping strain rate increases (or does not change), which shows the strain-hardening behavior of the specimens in the course of the test. Moreover, the results of the stepwise tests show that, with increase in the depth of the caves for gas storage, influence of the difference between minimum and maximum pressures on transient deformation of the rock increases.



Figure 3. UCS test using MTS testing machine equipped with lateral chained LVTD displacement sensors.

Table 1. Characteristics of the experimented cores in UCS test.

Sample code	L/D ratio	Purity of halite (%)	Crystal size (mm)
EU1	2.3	98	1-2.5
EU2	2.3	97	1-1.5
EU3	2.3	98	1-2
EU4	2.3	97	0.5-1.5
EU5	2.3	98	0.5-2

Table 2. Results of UCS test on the specimens.

Sample code	Density (g/cm <sup>3</sup> )	UCS (MPa)	E (GPa)	Poisson’s ratio
EU1	2.151	23.17	1.58	0.335
EU2	2.118	19.09	1.56	0.335
EU3	2.168	22.73	2.13	0.374
EU4	2.120	20.35	1.25	0.366
EU5	2.151	21.64	1.13	0.37
Average	2.142	21.4	1.5	0.36

**Table 3. Properties of the cores examined in LTC test.**

Sample code	L/D ratio	Stress (MPa)	Test time (days)
LTC1	2.32	5.5	20
LTC2	2.34	7.5	16
LTC3	2.34	10	26
LTC4	2.34	12	9
LTC5	2.32	14	9
LTC6	2.33	18	3

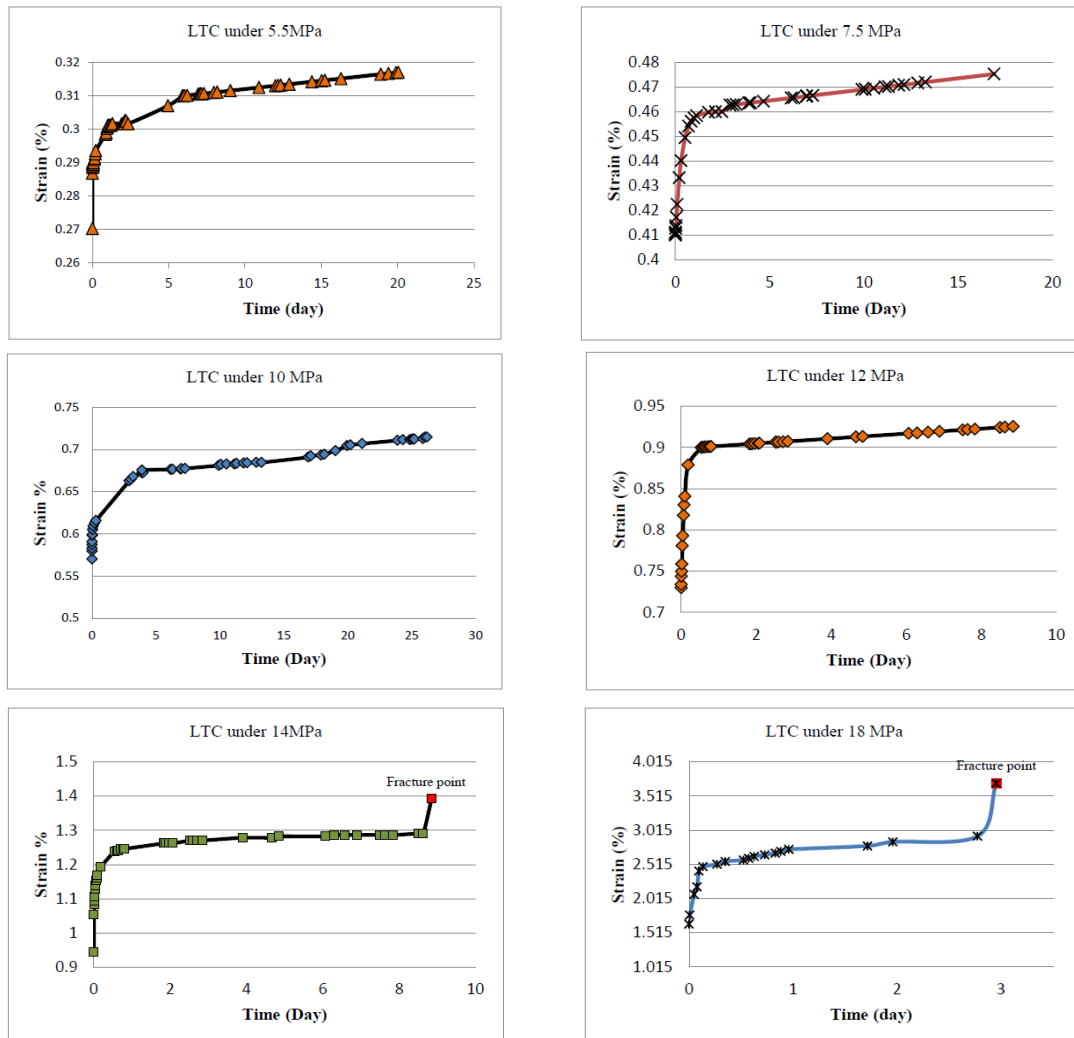


Figure 4. Results of LTC test at six different stresses.

**Table 4. Properties of the cores used in stepwise creep test.**

Sample code	L/D ratio	Level stress (MPa)	Test time (hour)
STC1	2.23	4.4 10.1 11.9	6.3
STC2	2.3	7.5 12 17	6.25

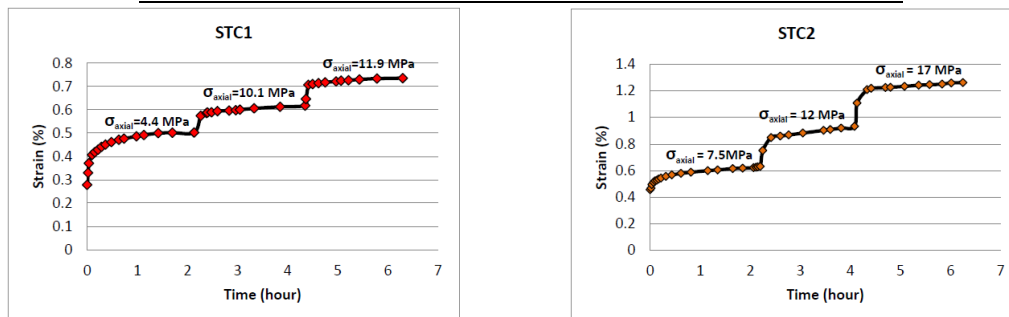


Figure 5. Results of stepwise creep tests on specimen STC1 and STC2.

### 3. Analysis of results of creep tests

As shown in Figure 6, the total strain under constant stress is equal to the elastic strain (instantaneous strain) and the creep strain (including the primary creep strain and the secondary creep strain), which is written as Equation 5:

$$\varepsilon_{total} = \varepsilon_e + \varepsilon_c = \varepsilon_{in} + (\varepsilon_p + \varepsilon_s) \quad (5)$$

where  $\varepsilon_e$  is the elastic strain and  $\varepsilon_c$  is the creep strain.  $\varepsilon_{in}$ ,  $\varepsilon_p$  and  $\varepsilon_s$  are the instantaneous strain, primary creep strain, and secondary creep strain, respectively.

In the present research work, the creep parameters were calculated using linear and non-linear (exponential) regression techniques on the test data. The calculated parameters were then validated using the parameters computed based on the Lubby 2 constitutive law.

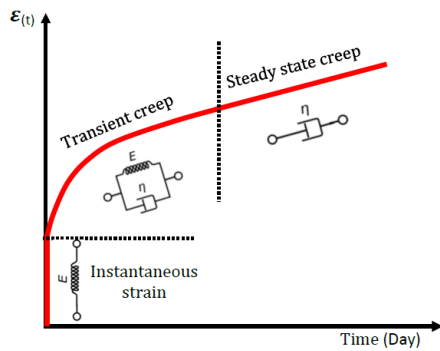


Figure 6. General creep curve obtained from creep tests on rock salt [4].

#### 3.1. Determination of creep parameters using Burger's rheological model

In order to determine the Maxwell's viscosity coefficient as a function of the applied stress to rock salt, the stationary portions of LTC test results were used. In the secondary creep stage (steady-state), the creep rate reaches a constant value ( $\frac{\sigma}{\eta_M}$ ). According to Figure 7, slope of the asymptote associated with steady-state creep indicates the steady-state strain rate of the creep, as the following equation:

$$\varepsilon = \frac{\sigma}{\eta_M} t + \varepsilon_0 \quad (6)$$

where  $\varepsilon$  is the time-dependent strain,  $\frac{\sigma}{\eta_M}$  is the steady-state strain rate of the rock salt,  $\varepsilon_0$  is the strain incurred at the intersection point of the

asymptote line of steady-state strain with strain axis,  $\sigma$  is the constant stress applied during the test,  $\eta_M$  is the Maxwell's viscoplastic coefficient, and  $t$  is time. The secondary creep behavior is due to the balance between the work-hardening and recovery processes [28].

The strain rate of the steady-state creep portion is defined as the quotient of the differential strain (i.e. total transient strain,  $\varepsilon_{tr}$ , is subtracted from the total creep strain,  $\varepsilon_t$ ) and the differential time (i.e. time of total transient strain,  $t_{tr}$ , is subtracted from the time of total creep strain,  $t_t$ ) in accordance with Eq. (7):

$$\dot{\varepsilon} = \frac{\Delta\varepsilon}{\Delta t} = \frac{\varepsilon_t - \varepsilon_{tr}}{t_t - t_{tr}} \quad (7)$$

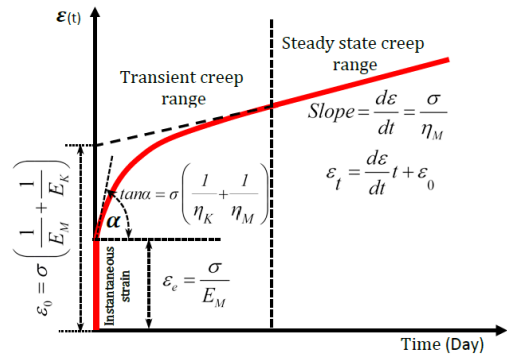


Figure 7. Properties of strain-time curve for determining creep parameters [28].

Therefore, the equation of the asymptote lines associated with the steady-state creep portion of each LTC test was obtained using linear regression. Afterwards, the equation obtained from the asymptote lines was compared to the linear Eq. (8), and the steady state strain rate of the rock salt was calculated for each LTC test. Subsequently, one may proceed to obtain the viscoplastic coefficient of each test from the following equation:

$$\dot{\varepsilon} = \frac{1}{\eta_M} \sigma \Rightarrow \eta_M = \frac{\sigma}{\dot{\varepsilon}} \quad (8)$$

The total transient strain, total strain stationary creep strain rate, and Maxwell's viscosity coefficient are reported in Table 5.

Since all the LTC tests were performed at the same constant temperature, there was no dependency between the Maxwell's viscosity coefficient and temperature. The Maxwell's viscosity coefficient was rather just stress-dependent.

**Table 5. Values of Maxwell’s viscosity coefficient for LTC tests.**

Stress value of LTC test (MPa)	Total transient strain	Total strain	Strain rate	$\bar{\eta}_M(\sigma)$ (MPa.d)
5.5	0.00307	0.00317	5.27E-6	1043643
7.5	0.004635	0.004752	9E-6	833333
10	0.006645	0.007145	20E-6	500000
12	0.0091	0.00925	33E-06	363636
14	0.0124	0.0129	60E-6	233333
18	0.0252	0.037	300E-06	90000

Using the exponential regression of viscoplastic coefficient values of the rock salt with respect to the different stress levels for each one of the conducted LTC tests in this research work, the exponential Eq. (9) was obtained as follows:

$$\bar{\eta}_{M(\sigma)} = (4 \times 10^6) \exp(-0.224\sigma) \quad (9)$$

Since the loading mechanism in the stepwise STC and LTC tests was all of sudden, we would have an instantaneous strain at the approximate time  $t = 0$ , i.e. at the beginning of all tests. The instantaneous strain depends on different levels of the applied load or stress. According to Figure 8, the value for  $\frac{\sigma}{E_M}$ , which refers to the instantaneous strain, will give the Maxwell’s elastic coefficient for each stepwise STC and LTC test. The results are presented in Table 6.

Figure 8 shows the non-linear correlation between instantaneous strain and different levels of stress as a power function (10):

$$\varepsilon_{in} = 0.0003\sigma^{1.33} \quad (10)$$

Furthermore, the value for  $\frac{\sigma}{E_K}$  was obtained by

subtracting the instantaneous or elastic strain from the strain incurred at the intersection point of the asymptote line with strain axis,  $\varepsilon_0$ . One may proceed to obtain the Kelvin’s elastic coefficient,  $E_K$ , of each stepwise STC and LTC test from the following equation:

$$\frac{\sigma}{E_K} = \varepsilon_0 - \varepsilon_e = \sigma \left( \frac{1}{E_K} + \frac{1}{E_M} \right) - \frac{1}{E_M} \quad (11)$$

The values of the Kelvin’s elastic coefficient for each stepwise STC and LTC tests are presented in Table 7.

**Table 6. Values of Maxwell’s elastic coefficient for each stepwise STC and LTC tests.**

Test type	Stress value (MPa)	Instantaneous strain or $\frac{\sigma}{E_M}$
LTC1	5.5	0.0027
LTC2	7.5	0.0041
LTC3	10	0.0057
LTC4	12	0.0073
LTC5	14	0.0098
LTC6	18	0.0141
Stepwise STC1	4.4	0.0022
	10.1	0.0059
	11.9	0.0068
Stepwise STC2	7.5	0.0045
	12	0.0075
	17	0.012

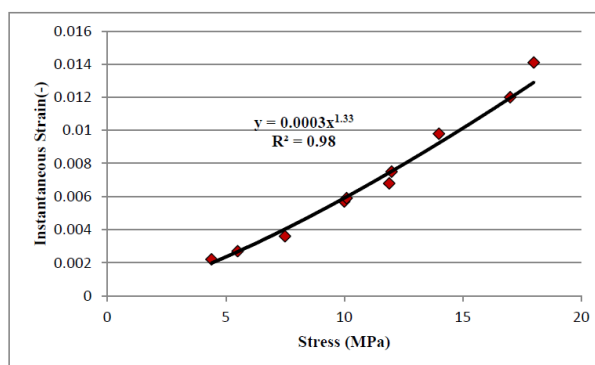


**Figure 8. Non-linear regression between instantaneous strain and different stress levels.**

According to the values for the Kelvin’s elastic coefficient in Table 7, using the exponential regression of for the Kelvin’s elastic coefficient of the rock salt with respect to the different stress levels for the conducted LTC tests in this research work, the exponential Eq. (12) is obtained:

$$\overline{E_{K(\sigma)}} = 63356 \exp(-0.18\sigma) \tag{12}$$

Given that the strain-time curves of the creep tests follow the Burger’s rheological model, the total strain can be calculated according to the Burger’s rheological model, as follows:

$$\varepsilon = \frac{\sigma}{E_M} + \frac{\sigma}{E_K} \left[ 1 - \exp\left(-\frac{E_K}{\eta_K} t\right) \right] + \frac{\sigma}{\eta_M} t \tag{13}$$

where  $\eta_K$  is the Kelvin’s viscoelastic coefficient, and the other parameters have been previously defined.

This model is a combination of the Maxwell spring, Kelvin body, and Maxwell dashpot, which

are attached together in series, as shown in Figure 6. For more details, please refer to [28].

The value for the Kelvin’s viscosity coefficient,  $\eta_K$ , at each stress level can be determined by selecting a specific time and corresponding the strain to that time from the creep curve within the transient creep region and substituting these values into Eq. (13). On this basis, the values for the Kelvin’s viscosity coefficient of each one of the stepwise STC and LTC tests are reported in Table 8.

Applying the exponential regression on the values obtained for the Kelvin’s viscosity coefficient of the rock salt at different stress levels of each one of the stepwise STC and LTC tests, one can end up with Eq. (14):

$$\overline{\eta_{K(\sigma)}} = 700 \exp(-0.15\sigma) \tag{14}$$

**Table 7. Values for Kelvin’s elastic coefficient for each stepwise STC and LTC test.**

Test type	Stress value (MPa)	$\varepsilon_0$	$\varepsilon_e$	$\frac{\sigma}{E_K}$	$E_K$ (MPa)
LTC1	5.5	0.00305	0.0027	0.00037	15714
LTC2	7.5	0.0041	0.0036	0.0005	15000
LTC3	10	0.0066	0.0057	0.0009	11111
LTC4	12	0.009	0.0075	0.0015	8000
LTC5	14	0.0125	0.0098	0.0027	5270
LTC6	18	0.0242	0.0164	0.0078	2308
Stepwise STC1	4.4	0.0046	0.0028	0.0003	28704
	10.1	0.006	0.00574	0.00026	10114
	11.9	0.0071	0.0064	0.0007	7276
Stepwise STC2	7.5	0.0088	0.00456	0.0042	16277
	12	0.0113	0.0088	0.0025	7144
	17	0.0126	0.012	0.0006	2861

**Table 8. Values for Kelvin’s viscosity coefficient for each stepwise STC and LTC test.**

Test type	Stress value (MPa)	Specific time (day)	Specific strain (mm/mm)	$\eta_K$ (MPa.d)
LTC1	5.5	0.017361	0.002395	247
LTC2	7.5	0.01875	0.004128	207
LTC3	10	0.01875	0.006312	183
LTC4	12	0.0166667	0.007587932	149
LTC5	14	0.016667	0.01108	134
LTC6	18	0.0069	0.01776	25
Stepwise STC1	4.4	0.016667	0.0033	273
	10.1	0.1333	0.0057	175
	11.9	0.016667	0.0065	152
Stepwise STC2	7.5	0.016667	0.0072	211
	12	0.05	0.0111	162
	17	0.05	0.0121	49

**3.2. Determination of creep parameters using LUBBY2 constitutive model**

The Lubby 2 constitutive model has the same structure as the Burgers model. This means that its mechanical components are made up of the Kelvin and Maxwell models, with the difference that their variables have for a non-linear relationship with stress. This model simulates both the transient (primary stage) and the stationary (secondary stage) creeps well but does not have the ability to describe the behavior of the accelerated creep (tertiary stage). Using this model, the stage-by-stage deformation of the material can be modeled. The Lubby 2 constitutive model has the ability to predict a negative strain rate (reverse creep) proportional to the unloading rate, which will guide the operation of caverns in the simulation of the injection and withdrawal cycles. On the other hand, in modeling the stepwise creep of materials, the dispersion and the fluctuations of data due to the difference in the mechanical properties of materials is largely eliminated. This model is considered as one of the suitable models for assessing the creeping behavior of salt rock, and has been used to predict its long-term behavior [29-32].

The mathematical relations 15 and 16 describe the behavior of materials by this model. Relation 15 is used to describe the strain of the time function, and relation 16 to describe the stationary strain trajectory of the material. The total rate of strain in this model is obtained by the additive superposition of the transient creep (primary stage) strain and steady creep (secondary stage) strain. This model presents the primary creep strain rate by either the time-hardening equation (Eq. (15)) or the strain-hardening equation (Eq. (16)) [29-32].

$$\dot{\epsilon}_{(t)} = \left[ \frac{1}{\eta_K(\sigma)} \exp\left(-\frac{\bar{G}_k(\sigma)}{\eta_K(\sigma)} t\right) + \frac{1}{\eta_M(\sigma)} \right] \times \sigma \quad (15)$$

$$\dot{\epsilon}_{(\epsilon_c)} = \left[ \frac{1}{\eta_K(\sigma)} \left( 1 - \frac{\epsilon_e \bar{G}_k(\sigma)}{\sigma} \right) + \frac{1}{\eta_M(\sigma)} \right] \times \sigma \quad (16)$$

The parameters in the above equations have been previously defined. In case the temperature remains constant in a test, there would be no dependency between the creep parameters of the Lubby 2 model and temperature. Thus, the creep parameters are dependent on stress in such cases. For further information, please refer to [29-32]. The creep parameters in Lubby 2 constitutive model are calculated as follow:

**3.2.1. Determining stationary creep parameter**

As described in sub-section 3.1, the Maxwell's viscosity coefficient is inversely proportional to the strain rate,  $\dot{\epsilon}_{(l)}^{st}$ , and has a direct relation with stress,  $\sigma_V$ , which is written as follows [29-32]:

$$\bar{\eta}_M(\sigma) = \frac{\sigma_V}{\dot{\epsilon}_{(l)}^{st}} \quad (17)$$

The strain rate is obtained from the asymptotic slope in the stable creep region. In the Lubby 2 model, the relationship between the Maxwell's viscosity coefficient and the various stress levels is expressed as Eq. (18) [29-32]:

$$\bar{\eta}_M(\sigma) = \bar{\eta}_M^* \exp(m \cdot \sigma) \quad (18)$$

Figure 9 demonstrates the exponential relationship between the Maxwell's viscoplastic coefficient and the stress levels. According to this figure, by non-linear regression of the data in the domain of  $\bar{\eta}_M - \sigma$ , the m and  $\bar{\eta}_M^*$  values in Eq. (18) were obtained as -0.2 and 4,000,000 MPa.day, respectively. On this basis, the Maxwell's viscoplastic coefficient as a function of the stress applied to the rock salt was obtained as follows:

$$\bar{\eta}_M(\sigma) = (4 \times 10^6) \exp(-0.2\sigma) \quad (19)$$

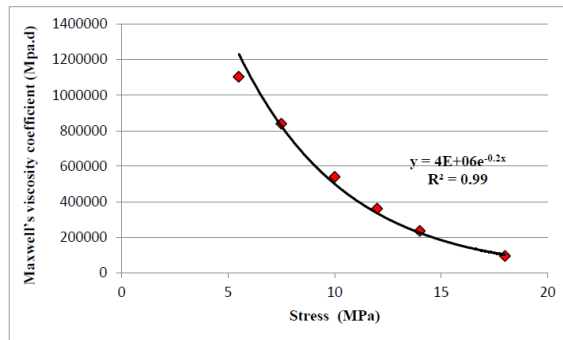


Figure 9. Nonlinear regression between Maxwell's viscoplastic coefficient and different stress levels.

**3.2.2. Determining primary creep parameters**

In order to describe the primary creep in the Lubby 2 model, the parameters  $\overline{G}_k^*$ ,  $k_1$ ,  $\overline{\eta}_K^*$  and  $k_2$  should be determined. The Kelvin’s shear modulus is inversely proportional to the transient strain,  $\dot{\varepsilon}_i^{st}$ , and has a direct relation with stress,  $\sigma_V$ , which is written as follows [29-32]:

$$\overline{G}_k(\sigma) = \frac{\sigma_V}{\varepsilon_i^{tr}} \tag{20}$$

where  $\sigma_V$  is the stress and  $\varepsilon_i^{tr}$  is the transient creep strain.

In a given stress, the Kelvin’s shear modulus decreases with increase in the transient strain. The transient portion of the creep strain is obtained by Eq. (21) [29, 32]:

$$\varepsilon_i^{tr} = \varepsilon_i^t - \varepsilon_{el} - \varepsilon_i^{\bullet st} \cdot \Delta t \tag{21}$$

where  $\varepsilon_i^t$  is the total creep strain,  $\varepsilon_{el}$  is the elastic strain resulting from the deviator load,  $\varepsilon_i^{\bullet st}$  is the rate of stationary creep strain, and  $\Delta t$  is the duration of the loading stage.

In the Lubby 2 model, the relationship between the Kelvin’s shear modulus and the various stress levels is expressed as Eq. (22) [29-32]:

$$\overline{G}_{k(\sigma)} = \overline{G}_k^* \exp(k_1 \sigma) \tag{22}$$

According to Figure 10, applying nonlinear regression of the data in  $\overline{G}_k - \sigma$  space, the parameters  $\overline{G}_k^*$  and  $k_1$  of the general Eq. (23) were obtained as -0.174 and 52228 MPa, respectively. On this basis, the Kelvin’s shear modulus as a function of the applied stress to rock salt is obtained as follows:

$$\overline{G}_k(\sigma) = 52228 \exp(-0.174\sigma) \tag{23}$$

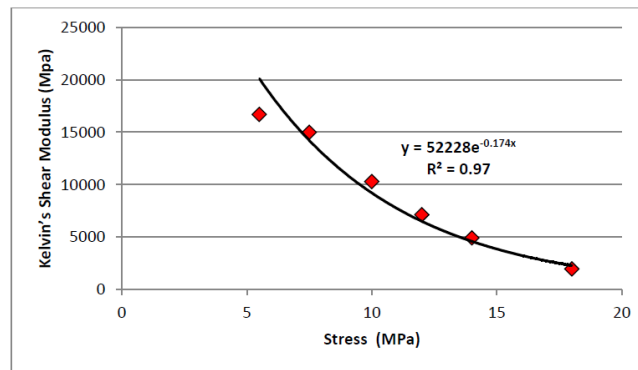


**Figure 10. Non-linear regression between Kelvin’s shear modulus and different stress levels.**

Also the Kelvin’s viscous modulus (or Kelvin’s viscoelastic coefficient) depends on the Kelvin’s shear modulus, equivalent stress, and transient creep strain (strain-hardening method). This coefficient,  $\overline{\eta}_K(\sigma)$ , is calculated using the following equation by removing the stationary stage creep equation [29, 32]:

$$\overline{\eta}_{K(\sigma)} = - \frac{\overline{G}_{k(\sigma)} \cdot t}{\ln(1 - \varepsilon_i^{tr} \cdot \frac{\overline{G}_{k(\sigma)}}{\sigma})} \tag{24}$$

The value for the transient creep strain ( $\varepsilon_i^{tr}$ ) is equal to the value of the total creep strain from the creep test curve at a specific point in time minus the value for the stationary creep strain calculated at that point.

The relation between the Kelvin’s viscous coefficient and the equivalent stress is represented as the exponential Eq. (25) [29-32]:

$$\overline{\eta}_{k(\sigma)} = \overline{\eta}_k^* \exp(k_2 \sigma) \tag{25}$$

According to Figure 11, applying the non-linear regression of Kelvin’s viscous coefficient values for each one of the stepwise STC and LTC tests (as obtained from Eq. (24)) in  $\overline{\eta}_k - \sigma$  space, the parameters  $\overline{\eta}_k^*$  and  $k_2$  of the general Eq. (25) were obtained as -0.38 and 68504 MPa.day, respectively.

Hence, the Kelvin’s viscous coefficient as a function of stress of rock salt is obtained as Eq. (26):

$$\overline{\eta}_{K(\sigma)} = 68504 \exp(-0.38\sigma) \tag{26}$$

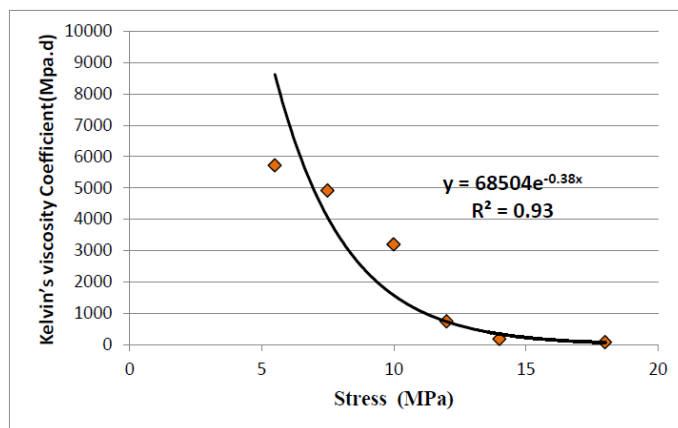


Figure 11. Non-linear regression between Kelvin’s viscosity coefficient and different stress levels.

**4. Presenting an experimental creep model based on linear and non-linear regression analyses**

Taking into account the form of strain-time curves for each one of the LTC and stepwise STC tests and fitting them to mathematical functions, the following general mathematical equation is proposed:

$$\epsilon = A + B(1 - e^{-Ct}) + Dt \tag{27}$$

where A, B, C, and D, are the parameters that are related to the creep properties of the rock salt and can be determined via experimental tests.

In order to calculate the constant parameters A, B, C, and D in Eq. (27), one should obtain the mathematical equations for the strain-time curves of each one of the LTC and stepwise STC tests by linearly and non-linearly regression of the data. On this basis, the linear regression of the data in the stationary creep range and non-linear regression of the data in the transient creep range on the strain-time curves obtained from the creep tests were performed using the  $\Sigma$ plot software.

The results of the linear and non-linear regression analyses on the data from each one of the LTC tests are given in Table 9.

Since the stepwise STC tests were only used for calculating the viscoelastic coefficient and the Kelvin’s shear modulus, so that the tests had no long stationary creep phase, then all of the values obtained from each phase of STC tests were included in the non-linear regression analysis. The results of the non-linear analysis of STC tests are given in Table 10.

The values for the parameters mentioned in Eq. (27) were obtained using the non-linear regression analysis. In order to calculate the parameters A, B, and C, the transient creep equations in Tables 9 and 10 of the SCT and LTC tests were used. However, to calculate parameter D, the stationary creep equations in Table 9 for the LTC tests were used. Based on the nonlinear regression analysis results, the squared correlation coefficients obtained in the fitting process were all greater than 0.90. Table 11 presents the results obtained by the  $\Sigma$ plot software.

**Table 9. Results of the linear and non-linear regression analyses on the data from each one of the LTC tests.**

Stress value of LTC test (MPa)	Non-linear regression equation in transient creep zone	Linear regression equations in stationary creep zone
5.5	$\epsilon_{tr} = 0.0027 + 0.00035(1 - e^{-(1.77t)})$ $R^2 = 0.96$	$\epsilon_{st} = (5.27E-6)t + 0.00244$ $R^2 = 0.95$
7.5	$\epsilon_{tr} = 0.0041 + 0.0005(1 - e^{-(3.1t)})$ $R^2 = 0.97$	$\epsilon_{st} = (9E-6)t + 0.004$ $R^2 = 0.93$
10	$\epsilon_{tr} = 0.0057 + 0.001(1 - e^{-(5.2t)})$ $R^2 = 0.95$	$\epsilon_{st} = (20E-6)t + 0.00662$ $R^2 = 0.97$
12	$\epsilon_{tr} = 0.0073 + 0.0017(1 - e^{-(11.2t)})$ $R^2 = 0.96$	$\epsilon_{st} = (33E-6)t + 0.009$ $R^2 = 0.98$
14	$\epsilon_{tr} = 0.0098 + 0.0029(1 - e^{-(18.8t)})$ $R^2 = 0.91$	$\epsilon_{st} = (60E-6)t + 0.01246$ $R^2 = 0.92$
18	$\epsilon_{tr} = 0.0164 + 0.0089(1 - e^{-(25t)})$ $R^2 = 0.93$	$\epsilon_{st} = 0.0003t + 0.0242$ $R^2 = 0.94$

**Table 10. Results of non-linear regression of the data from each stepwise STC test.**

Creep test method	Non-linear regression equation for transient creep zone	
Stepwise STC (MPa)	4.4	$\epsilon_{tr} = 0.0022 + 0.0002(1 - e^{(-1.24t)})$ $R^2 = 0.96$
	10.1	$\epsilon_{tr} = 0.0057 + 0.001(1 - e^{(-5.1t)})$ $R^2 = 0.97$
	11.9	$\epsilon_{tr} = 0.0065 + 0.0016(1 - e^{(-11t)})$ $R^2 = 0.95$
Stepwise STC (MPa)	7.5	$\epsilon_{tr} = 0.0047 + 0.0005(1 - e^{(-3t)})$ $R^2 = 0.97$
	12	$\epsilon_{tr} = 0.0068 + 0.002(1 - e^{(-11.1t)})$ $R^2 = 0.99$
	17	$\epsilon_{tr} = 0.012 + 0.007(1 - e^{(-22.9t)})$ $R^2 = 0.98$

**Table 11. Parameters of the proposed creep model.**

Parameters	Equation	R <sup>2</sup>
A	$0.0003\sigma^{1.33}$	0.93
B	$(6E - 5)e^{0.28\sigma}$	0.95
C	$(0.52)e^{0.23\sigma}$	0.91
D	$(0.8E - 6)e^{0.32\sigma}$	0.98

**5. Comparison between experimental creep model and adjusted Lubby 2 constitutive model**

For the sake of validation, the obtained experimental model was compared with the Lubby 2 constitutive model at different levels of stress (5.5, 7.5, 10, 12, 14 and 18 MPa). The results of this comparison are presented in Figure 12. As it can be seen in this figure, there is a good agreement between the results of the empirical model and those calculated based on the Lubby 2 model as well as the creep tests data. Given that the stationary and accelerated creep zones are of particular importance in designing, construction, and operation of underground spaces, the present model can very well model instantaneous (elastic) strain, transient creep zone, and, in particular,

stable creep zone. The slight difference between the empirical model results and test data, on one hand, and the Lubby 2 model results, on the other hand, is related to the regression and calculation errors. Comparison of the test values with the model curves indicated that they were nearly identical, verifying that the proposed creep model could accurately describe the creep properties of rock salt under uniaxial compressive stress. It was also observed that in the low stress levels (5.5 and 7.5 MPa), the proposed experimental model had a better fit on the experimental data than the Lubby 2 model. This is due to changes in the values for the Kelvin’s elastic modulus and the Kelvin’s viscous coefficient.

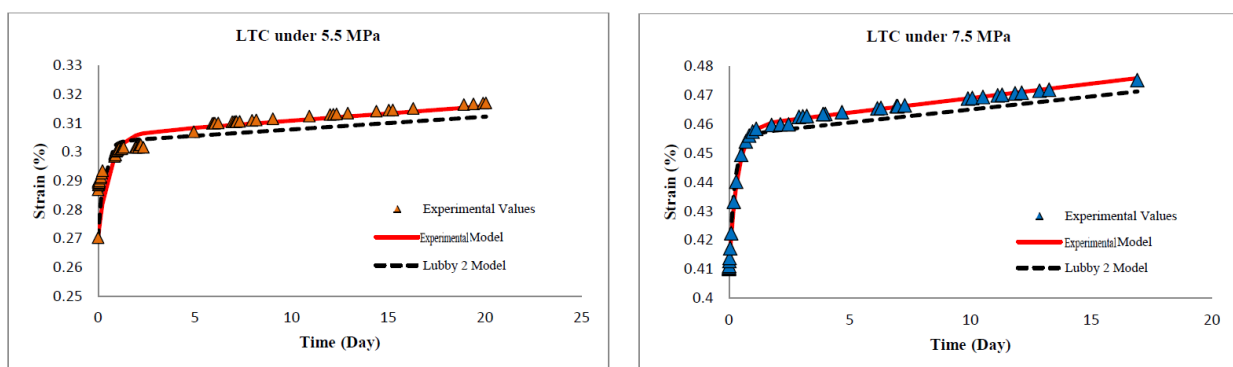


**Figure 12. Comparison between empirical model and Lubby 2 constitutive law as well as the data obtained from LTC tests at different stresses.**

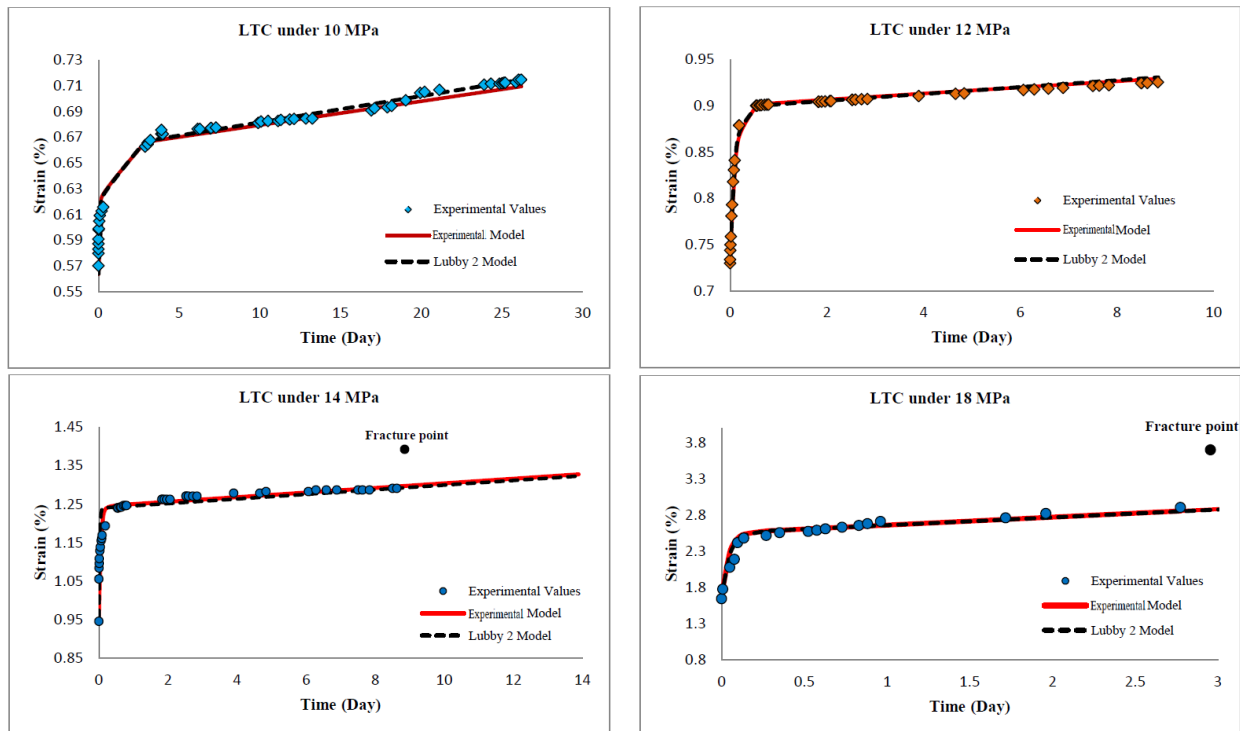


Figure 12. Continued.

## 6. Conclusions

- The results obtained for the long-term creep tests show that the level of stress applied to the specimen impose a direct impact on the stationary creep rate of the rock. In other words, as underground spaces go deeper, spatial convergence increases exponentially.

- Based on the results obtained from the LTC and stepwise STC tests, it can be stipulated that the general and original deformations in the rock salt specimens are a function of the stress history. However, the deformation (strain) occurring in the stationary creep phase is independent from the stress history and is rather controlled by the current stress field within the rock salt.

- Given that the loading mechanism at the beginning of the creep tests was instantaneous, an instantaneous strain would be expected in each one of the creep tests. As such, in the present research work, the relationship between instantaneous strains and different levels of stress were obtained using non-linear regression in the form of the power function  $\varepsilon = 0.0003\sigma^{1.33}$ .

- Based on the linear and non-linear regression analyses of the data obtained from the LTC and stepwise STC tests, an experimental model was presented in accordance with (27). The proposed experimental model exhibited a good agreement with the STC and LTC test values at a determination factor of 93%.

- With the proposed model, we can obtain the strain-time curve and creep coefficients at different levels of stress (other than the tests performed) in the range of 18-18 MPa. As such, this model is evaluated as valid and reliable for determining the values for the strain at different levels of stress, particularly in the range of 4-18 MPa.

- This model is used to calibrate the creep parameters of the Lubby 2 constitutive model.

- Based on the adjusted Lubby 2 constitutive model, the viscoelastic moduli and the Kelvin's shear modulus of the stress function of the rock were determined as the exponential functions  $\overline{\eta}_K(\sigma) = 68504 \exp(-0.38\sigma)$  and  $\overline{G}_k(\sigma) = 52228 \exp(-0.174\sigma)$ , respectively.

- Moreover, the viscoplastic coefficient of the stress function of rock salt was obtained, based on the LTC tests, as the exponential relation  $\overline{\eta}_M(\sigma) = (4 \times 10^6) \exp(-0.2\sigma)$ .

## Acknowledgments

The experiments were carried out in the rock mechanic laboratory of the School of Mining at the University of Tehran. The authors are grateful for the favor and cooperation of the authorities, especially Mr. Ebdali who helped us in the preparation of the rock salt specimens.

## References

- [1]. Senseny, P.E., Handin, J.W., Hansen, F.D. and Russell, J.E. (1992). Mechanical behavior of rock salt: phenomenology and micro-mechanisms. *International Journal of Rock Mechanics and Mining Sciences*. 29 (4): 363-378.
- [2]. Ito, T. and Akagi, T. (2001). Methods to predict the time of creep failure, *Proceedings of the 31<sup>st</sup> Symposium on Rock Mechanics of Japan*. pp. 77-81.
- [3]. Bles, J. and Feuga, B. (1986). *The Fracture of Rocks*, published by: New York, North Oxford Academic Publisher Ltd.
- [4]. Goodman, R.E. (1989). *Introduction to Rock Mechanics*, 2<sup>nd</sup> ed., John Wiley & Sons, New York.
- [5]. Jeremic, M.L. (1994). *Rock mechanics in salt mining*. Netherland: Balkema. 544 P.
- [6]. Aydan, O., Ito, T., Ozbay, U., Kwasniewski, M.A., Shahriar, K., Okuno, T., Ozgenoglu, A. and Malan, D.F. (2014). ISRM Suggested methods for determining the creep characteristics of rock. Hacettepe University, Department of Geological Engineering, 06800 Beytepe, Ankara, Turkey.
- [7]. Liang, W.G., Zhang, C.A., Gao, H.G., Yang, X.Q., Xu, S.G. and Zhao, Y.S. (2011). Experiments on mechanical properties of rock salts under cyclic loading. *Journal of Rock Mechanics and Geotechnical Engineering*. 4 (1): 54-61.
- [8]. Fuenkajorn, K. and Phueakphum, D. (2009). Effects of Cyclic Loading on the Mechanical Properties of Maha Sarakham Salt. 2, Thailand. *Suranaree Journal of Science and Technology*. 16: 91-102.
- [9]. Ishizuka, Y., Koyama, H. and Komura, S. (1993). Effect of strain rate on strength and frequency dependence of fatigue failure of rocks. *Assessment and Prevention of Failure Phenomena in rock Engineering*. pp. 321-327.
- [10]. Langer, M. (1984). The Rheological Behaviour of Rock Salt, In *Proceedings of the First Conference on the Mechanical Behavior of Salt, Clausthal-Zellerfeld*, Trans Tech Publications. pp. 201-240.
- [11]. Khathiphathee, T. (2012). Effects of low temperatures on strength and time-dependent deformation of rock salt. Master Degree Thesis, Suranaree University of Technology, NakhonRatchasima, Thailand.
- [12]. Hagros, A., Johanson, E. and Hudson, J.A. (2008). Time dependency in the mechanical properties of crystalline rocks, a literature survey. *Possiva OY, Finland*.
- [13]. Raj, S.V. and Pharr, G.M. (1992). Effect of temperature on the formation of creep substructure in sodium chloride single crystal. *American Ceramic Society*. 75 (2): 347-352.
- [14]. Wawersik, W.R. (1988). Alternatives to a power-law creep model for rock salt at temperatures below 160 °C, In *Proceedings of the Second Conference on the Mechanical Behavior of Salt Clausthal-Zellerfeld*, Trans Tech Publications. pp. 103-126.
- [15]. Munson, D.E. and Dawson, P.R. (1984). Salt Constitutive Modeling Using Mechanism Maps, In *Proceedings of the First Conference on the Mechanics Behavior of Salt, Clausthal-Zellerfeld*, Trans Tech Publications. pp. 717-737.
- [16]. Hunsche, U. and Schulze, O. (1996). Effect of humidity and confining pressure on creep of rock salt, In *Proceedings of the Third Conference on the Mechanical Behavior of Salt, Clausthal-Zellerfeld*: Trans Tech Publications. pp. 237-248.
- [17]. Urai, J.L. and Spiers, C.J. (2007). The effect of grain boundary water on deformation mechanisms and rheology of rock salt during long-term deformation. *Proceedings of the 6<sup>th</sup> conference on the mechanical behavior of salt, Hannover, Germany*. 22-25 May.
- [18]. Franssen, R.C.M. (1998). Mechanical anisotropy of synthetic polycrystalline rock salt, In *Proceedings of the Fourth Conference on the Mechanical Behavior of Salt, Clausthal-Zellerfeld*, Trans Tech Publications. pp. 63-75.
- [19]. Hamami, M., Tijani, S.M. and Vouille, G. (1996). A methodology for the identification of rock salt behavior using multi-step creep tests, In *Proceedings of the Third Conference on the Mechanical Behavior of Salt, Clausthal-Zellerfeld*: Trans Tech Publications. pp. 53-66.
- [20]. Mirza, U.A. (1984). Prediction of creep deformations in rock salt pillars, In *Proceedings of the First Conference on the Mechanical Behavior of Salt, Clausthal-Zellerfeld*, Trans Tech Publications. pp. 311-337.
- [21]. Moghadam, S.N., Mirzabozorg, H. and Noorzad, A. (2013). Modeling time-dependent behavior of gas caverns in rock salt considering creep, dilatancy and failure. *Tunn Undergr Space Technol*. 33: 171-185.
- [22]. Liu, X., Yang, X. and Wang, J. (2015). A nonlinear creep model of rock salt and its numerical implement in FLAC3D. *Adv Mater Sci Eng*. 8 pages. <https://doi.org/10.1155/2015/285158>.
- [23]. Minkley, W. and Muhlbauer, J. (2007). Constitutive models to describe the mechanical behavior of salt rocks and the imbedded weakness planes. In *6<sup>th</sup> Conference on the Mechanical Behavior of Salt, Hannover, Germany*. pp. 22-25.
- [24]. Fahimifar, A.H., Karami, M. and Fahimifar, A.S. (2015). Modifications to an elasto-visco-plastic constitutive model for prediction of creep deformation of rock samples. *Soils Found*. 55 (6): 1364-1371.
- [25]. Ling, C.H., Besson, J., Forest, S., Tanguy, B., Latourte, F. and Bosso, E. (2016). An elasto-visco-

plastic model for porous single crystals at finite strains and its assessment based on unit cell simulations. *International Journal of Plasticity*. 84: 58-87.

[26]. Wang, G., Zhang, L., Zhang, Y. and Ding, G. (2014). Experimental investigations of the creep–damage–rupture behaviour of rock salt. *International Journal of Rock Mechanics & Mining Sciences*. 66: 181-187.

[27]. Khaledi, K., Mahmoudi, E., Datcheva, M., König, D. and Schanz, T. (2016). Sensitivity analysis and parameter identification of a time dependent constitutive model for rock salt. *Journal of Computational and Applied Mathematics*. 293: 128-138.

[28]. Houhou, N., Benzarti, K., Quiertant, M., Chataigner, S., Fléty, A. and Marty, C. (2012). Analysis of the Non-Linear Creep Behavior of FRP-Concrete Bonded Assemblies. *Journal of Adhesion Science and Technology*. DOI: 10.1080/01694243.2012.697387.

[29]. Heusermann, S., Rolfs, O. and Schmidt, U. (2003). Nonlinear finite-element analysis of solution mined storage cavern in rock salt using the LUBBY2 constitutive model. *Computer and Structures*. pp. 629-638.

[30]. Sereshki, F. and Saffari, A. (2016). Effects of Ratcheting Strain on Cyclic Time-Dependent Parameters of Salt Rocks. *International Journal of Mining Science (IJMS)*. 2 (1): 15-24.

[31]. Zhao, J., Hou, M.Z.H. and Xing, W. (2013). Parameter Determination for the Constitutive Model Lubby 2 and Strength Model Hou Based on Laboratory Tests on Rock Salt Samples from Jintan, P.R. China. *Proceedings of the 3<sup>rd</sup> Sino-German Conference. Underground Storage of CO<sub>2</sub> and Energy*. Goslar, Germany.

[32]. Lux, K.H. and Düsterloh, U. (2014). Experimental acute renal failure. *Laboratory Report Larne-Carnduff*. Chair for Waste Disposal Technologies and Geomechanics, Clausthal University of Technology, Germany.

## ارائه یک مدل خزش تجربی برای سنگ نمک

محمد باقر اسلامی اندارگلی<sup>۱</sup>، کوروش شهریار<sup>۲\*</sup>، احمد رمضان زاده<sup>۳</sup> و کامران گشتاسبی<sup>۴</sup>

۱- گروه مهندسی معدن، واحد علوم و تحقیقات، دانشگاه آزاد اسلامی، تهران، ایران

۲- دانشکده مهندسی معدن و متالورژی، دانشگاه صنعتی امیرکبیر، ایران

۳- دانشکده مهندسی معدن، نفت و ژئوفیزیک، دانشگاه صنعتی شاهرود، ایران

۴- بخش مهندسی معدن، دانشکده فنی و مهندسی، دانشگاه تربیت مدرس، ایران

ارسال ۲۰۱۷/۱۲/۲۰، پذیرش ۲۰۱۸/۵/۵

\* نویسنده مسئول مکاتبات: k.shahriar@aut.ac.ir

### چکیده:

در دهه‌های اخیر، طراحی و ساخت فضاهای زیرزمینی در سنگ نمک برای ذخیره‌سازی سیالات نفتی، گاز طبیعی و انرژی‌های فشرده و همچنین دفن زباله‌های اتمی و شیمیایی توجه ویژه‌ای شده است. سنگ نمک دربرگیرنده فضاهای یادشده، در طی ساخت و یا بهره‌برداری از آن‌ها تحت تأثیر انواع نیرو و یا تنش یکنواخت و تناوبی کوتاه مدت و بلند مدت قرار می‌گیرند. بر این اساس بررسی رفتار مکانیکی سنگ نمک تحت تأثیر عوامل مختلف فیزیکی و مکانیکی ضروری است. مهم‌ترین عوامل مؤثر بر رفتار خزشی سنگ نمک ترکیب کانی‌ها و اندازه بلورهای تشکیل‌دهنده‌ی سنگ نمک، رطوبت، دما، زمان، شیوه بارگذاری، نرخ بارگذاری، نرخ کرنش و مدت بارگذاری هستند. در بررسی حاضر، شیوه بارگذاری و مدت بارگذاری در نظر گرفته شده است. بر این اساس به منظور دستیابی به درک صحیحی از رفتار خزشی سنگ نمک، تعیین ضرایب خزشی از طریق آزمون‌های آزمایشگاهی ضروری است؛ بنابراین ۲۰ نمونه استوانه‌ای با نسبت طول به قطر بیش از ۲ برای انجام آزمایش‌های خزش آماده شدند. دو آزمایش خزش کوتاه مدت مرحله‌ای هر یک در سه سطح تنش به ترتیب ۴/۴، ۱۰/۱ و ۱۱/۹ مگا پاسکال و ۷/۵، ۱۲ و ۱۷ مگا پاسکال و ۸ آزمون خزش بلند مدت در شش سطح تنش ۵/۵، ۷/۵، ۱۰، ۱۲، ۱۴ و ۱۸ مگا پاسکالی انجام شدند. سپس، ابتدا ضرایب خزش بر اساس مدل بنیادی لابی ۲ تعیین شدند. ضرایب به دست آمده با استفاده از نتایج آزمون‌های خزش تنظیم شدند. سپس با استفاده از رگرسیون خطی و غیرخطی داده‌های آزمون‌های خزش یک مدل تجربی خزش ارائه شد. برای اعتبارسنجی نتایج به دست آمده، هم مدل بنیادی لابی ۲ اصلاح شده و هم مدل تجربی پیشنهادی با نتایج به دست آمده از آزمون‌های خزش مقایسه شدند. هر دو مدل تطبیق نسبتاً خوبی با داده‌های آزمون‌های خزش با ضریب تعیین ۹۳٪ داشتند.

**کلمات کلیدی:** سنگ نمک، آزمایش خزش، مدل تجربی، مدل لابی ۲، ضرایب خزش.